Inorg. Chem. **2008**, *47*, 9583−9591

High-Connectivity Networks and Hybrid Inorganic Rod Materials Built from Potassium and Rubidium *p*-Halide-Substituted Aryloxides

J. Jacob Morris, Bruce C. Noll, and Kenneth W. Henderson*

Department of Chemistry and Biochemistry, University of Notre Dame, Notre Dame, Indiana 46556

Received June 20, 2008

A series of complex networks have been synthesized from the association of potassium and rubidium *p*-halide-substituted aryloxides using 1,4-dioxane molecules as neutral linkers. The crystalline polymers $[(4\text{-F-}C_6H_4OK)_6\cdot(\text{dioxane})_4]_\infty$ (**1**), $[(4\text{-I-}C_6H_4OK)_6\cdot(\text{dioxane})_6]_\infty$ (**2**), and $[(4\text{-I-}C_6H_4ORb)_6\cdot(\text{dioxane})_6]_\infty$ (**3**) are built from discreet, hexameric M_6O_6 aggregates. Compound **1** forms an unusual 16-connected framework involving both K−F and K−O_{diox} interactions. Each hexamer connects to eight neighboring aggregates through double-bridging contacts, resulting in a body-centered cubic (**bcu**) topology. Compounds **2** and **3** are isostructural, 12-connected networks, where each aggregate utilizes six dioxane double bridges to form primitive cubic (**pcu**) nets. In contrast, the complexes $[(4\text{-Cl-}C_6H_4OK)_3\cdot(\text{dioxane})]_\infty$ (**4**), $[(4\text{-Br-}C_6H_4OK)_2\cdot(\text{dioxane})_{0.5}]_\infty$ (**5**), and $[(4\text{-Br-}C_6H_4ORb)_5\cdot(\text{dioxane})_5]_\infty$ (**6**) are built from one-dimensional (1D) inorganic rods composed solely of M−O_{Ar} interactions. The extended structures of both **4** and **5** can be described as **pcu** nets, where parallel 1D inorganic pillars are connected through dioxane bridges. Compound **6** is also composed of parallel 1D inorganic rods, but in this instance the coordinated dioxane molecules do not bridge, resulting in isolated, close-packed chains in the solid state.

Introduction

There is currently a great deal of interest in the synthesis and characterization of metal−organic frameworks and coordination polymers.[1] A common strategy for the synthesis of these materials is the building-block approach, in which isolated metal atoms or metal clusters are linked by bridging organic ligands.[2] In these materials, the metal centers or molecular aggregates act as zero-dimensional (0D) nodes, and the dimensionality of the extended structures is derived from connecting these points through organic ligands.[3] Although less common, networks can also be constructed from inorganic one-dimensional (1D) rods or two-dimensional (2D) sheets that are connected by polyfunctional organic ligands.[4] These materials are classified as extended organic−inorganic hybrids, where one or two of the total dimensions are composed solely of M−X−M bonding (where X = O, N, S, F, etc.).[5]

We have recently shown that preassembled lithium and sodium aryloxide aggregates may be used as secondary building units (SBUs) to direct the assembly of diamondoid and cubic nets.[6] These systems were designed such that specific solution aggregates could be obtained, where each metal has one or two coordination sites available for divergent Lewis base ligation. This approach compensates for the lack of directionality commonly associated with alkali

* To whom correspondence should be addressed. E-mail: khenders@nd.edu. Phone: 574-631-8025. Fax: 574-631-6652.

(1) (a) Janiak, C. *Dalton Trans.* **2003**, 2781. (b) Cheetham, A. K.; Rao, C. N. R.; Feller, R. K. *Chem. Commun. (Cambridge, U.K.)* **2006**, 4780. (c) Robin, A. Y.; Fromm, K. M. *Coord. Chem. Rev.* **2006**, *250*, 2127. (d) El-Kaderi, H. M.; Hunt, J. R.; Mendoza-Cortés, J. L.; Côté, A. P.; Taylor, R. E.; O'Keeffe, M.; Yaghi, O. M. *Science* **2007**, *316*, 268. (e) Fromm, K. M. *Coord. Chem. Rev.* **2008**, *252*, 856.

(2) Haiduc, I.; Edelmann, F. T. *Supramolecular Organometallic Chemistry*; Wiley-VHC: New York, 1999.

(3) Ockwig, N. W.; Delgado-Friedrichs, O.; O'Keeffe, M.; Yaghi, O. M. *Acc. Chem. Res.* **2005**, *38*, 176.

(4) Cheetham, A. K.; Rao, C. N. R.; Feller, R. K. *Chem. Commun.* **2006**, 4780.

(5) (a) Guillou, N.; Livage, C.; van Beek, W.; Nogues, M.; Férey, G. *Angew. Chem., Int. Ed.* **2003**, *42*, 644. (b) Rosi, N. L.; Kim, J.; Eddaoudi, M.; Chen, B.; O'Keeffe, M.; Yaghi, O. M. *J. Am. Chem. Soc.* **2005**, *127*, 1504. (c) Feller, R. K.; Cheetham, A. K. *Solid State Sci.* **2006**, *8*, 1121.

(6) (a) MacDougall, D. J.; Morris, J. J.; Noll, B. C.; Henderson, K. W. *Chem. Commun. (Cambridge, U.K.)* **2005**, 456. (b) MacDougall, D. J.; Noll, B. C.; Henderson, K. W. *Inorg. Chem.* **2005**, *44*, 1181. (c) Morris, J. J.; Noll, B. C.; Henderson, K. W. *Cryst. Growth Des.* **2006**, *6*, 1071. (d) Henderson, K. W.; Noll, B. C.; Kennedy, A. R.; MacDougall, D. J. *Dalton Trans.* **2006**, 1875.

10.1021/ic801140u CCC: $40.75
Published on Web 09/26/2008

metal ions.[7,8] Subsequently, we demonstrated that ring and cage aggregates, containing the large alkali metal potassium or rubidium, could be utilized as building blocks for the creation of high-connectivity nets.[9] In particular, these aggregates allow for multiple points of network connection as highlighted by the synthesis of two new types of seven-connected nets and the first reported example of a nine-connected net.[9] The formation of unusual network connectivities is a highly topical area.[10] Indeed, with the ever-growing number of extended solid-state materials being reported and an increasing array of structural types appearing, there has recently been a focus toward identifying and classifying the underlying topologies of extended solids. This systematic enumeration has been aided greatly by the construction of searchable databases and computer programs designed for topological analysis.[11]

Following our initial studies, we were attracted toward the use of the *p*-halide-substituted aryloxide ligands. We were interested in this class of substituted phenols for two reasons. First, the absence of a substituent at the *o*-position potentially allows for an increase in the number of $M-O_{solv}$ bonds that may lead to the formation of high-connectivity networks.[6,12] The second reason for further study is the potential of these systems to form network connections through the *p*-halide unit.[13] For example, our previously reported complex $[(4\text{-}F\text{-}C_6H_4ONa)_6\cdot(dioxane)_3]_\infty$ bonds through both $Na-O_{diox}$ and $Na-F_{Ar}$ interactions.[6b] The molecular unit of this complex is a hexameric Na_6O_6 aggregate, which is solvated by six, bridging dioxane molecules. Network expansion gives a three-dimensional (3D) network with primitive cubic (**pcu**) topology through the dioxane bridges. However, there are close interaggregate $Na-F_{Ar}$ interactions between neighboring hexamers (Figure 1). This increases the connectivity of the framework to eight, giving an extended net with hexagonal primitive (**hex**) topology. The formation of the $Na-F_{Ar}$ interactions prompted us to further study systems that could have this unusual type of interaction for network growth.

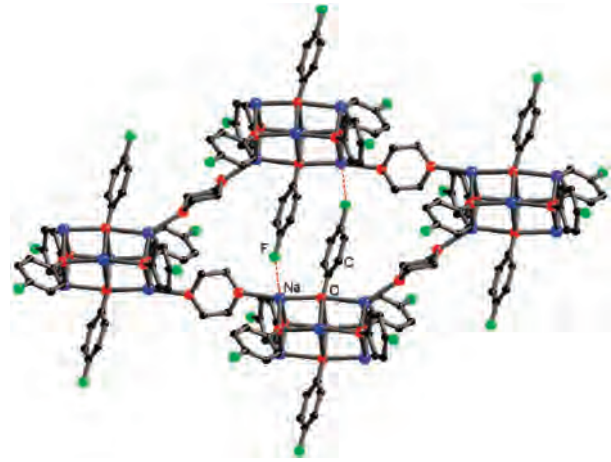

Figure 1. Section of the extended structure of $[(4\text{-}F\text{-}C_6H_4ONa)_6\cdot(dioxane)_3]_\infty$ showing network contacts through both dioxane and $Na-F_{Ar}$ bridges. Additional dioxane molecules and hydrogen atoms have been removed for clarity.

The work outlined here details the synthesis and structural characterization of dioxane-solvated polymeric materials produced from the combination of *p*-halide-substituted aryloxides with the large alkali metals potassium and rubidium.

Experimental Section

General Procedures. All experimental manipulations were performed under a dry nitrogen atmosphere using standard Schlenk techniques or in an argon-filled glovebox.[14] All glassware was flame-dried under vacuum before use. Hexane was dried immediately before use by passage through columns of a copper-based catalyst and alumina (Innovative Technology) and stored over 4 Å molecular sieves. Dioxane was purchased from Acros and was distilled over sodium benzophenone under N_2 prior to use. The phenols were purchased from Aldrich and were recrystallized from hexane. Potassium hexamethyldisilazide (KHMDS) was purchased from Aldrich and was used as received. $[^tBuORb\cdot{}^tBuOH]_\infty$ was prepared by literature methods.[15] d_6-DMSO was purchased from Cambridge Isotope Laboratories and was dried by storage over 4 Å molecular sieves. ^1H NMR spectra were recorded on a Bruker AVANCE DPX 400 spectrometer at 293 K and were referenced internally to the residual signals of the deuterated solvents. Elemental analyses and melting points were not attempted due to the potentially explosive nature of alkali metal derivatives of halide-substituted aromatics.[16] ^1H NMR spectroscopic studies of the isolated crystals indicated the partial removal of the dioxane solvent. Relative integral values for the remaining dioxane were dependent on the isolation conditions (time in vacuo, temperature, etc.) and, therefore, are not quoted.

X-ray Crystallography. Crystals were examined under Infineum V8512 oil. The datum crystal was affixed to a thin, glass fiber or MiTeGen micromount atop a tapered, copper mounting pin and transferred to the 100 K nitrogen stream of a Bruker APEX II

(7) For other examples of alkali metal aggregates used in network construction see: (a) Henderson, K. W.; Kennedy, A. R.; McKeown, A. E.; Strachan, D. *J. Chem. Soc., Dalton Trans.* **2000**, 4348. (b) Henderson, K. W.; Kennedy, A. R.; MacDougall, D. J.; Shanks, D. *Organometallics* **2002**, *21*, 606. (c) Henderson, K. W.; Kennedy, A. R.; Macdonald, L.; MacDougall, D. J. *Inorg. Chem.* **2003**, *42*, 2839. (d) Morris, J. J.; Noll, B. C.; Schultz, A. J.; Piccoli, P. M. B.; Henderson, K. W. *Inorg. Chem.* **2007**, *46*, 10473. (e) Morris, J. J.; Noll, B. C.; Honeyman, G. G.; Kennedy, A. R.; Mulvey, R. E.; Henderson, K. W. *Chem.—Eur. J.* **2007**, *13*, 4418. (f) Morris, J. J.; MacDougall, D. J.; Noll, B. C.; Henderson, K. W. *Dalton Trans.* **2008**, 3429.

(8) (a) Stey, T.; Stalke, D. In *The Chemistry of Organolithium Compounds*; Rappoport, Z., Patai, S., Eds.; Wiley: New York, 2004; Chapter 2. (b) Weiss, E. *Angew. Chem., Int. Ed. Engl.* **1993**, *32*, 1501. (c) *Lithium Chemistry, A Theoretical and Experimental Overview*; Sapse, A. M., Schleyer, P. v. R., Eds.; Wiley: New York, 1995.

(9) Morris, J. J.; Noll, B. C.; Henderson, K. W. *Chem. Commun. (Cambridge, U.K.)* **2007**, 5191.

(10) Hill, R. J.; Long, D. L.; Champness, N. R.; Hubberstey, P.; Schröder, M. *Acc. Chem. Res.* **2005**, *38*, 335.

(11) (a) O'Keeffe, M.; Yaghi, O. M.; Ramsden, S. Reticular Chemistry Structure Resource, Arizona State University: Tempe, AZ, 2006 http://rcsr.anu.edu.au. (b) Ramsden, S.; Robins, V.; Hyde, S. T.; Hungerford, S. EPINET: Euclidean Patterns in Non-Euclidean Tilings, 2006 http://epinet.anu.edu.au. (c) Blatov, V. A. 2007. http://www.topos.ssu.samara.ru. (d) Batten, S. R. http://www.chem.monash.edu.au/staff/sbatten/interpen/index.html.

(12) (a) Jackman, L. M.; Çizmeciyan, D. *Magn. Reson. Chem.* **1996**, *34*, 14. (b) Jackman, L. M.; Çizmeciyan, D.; Williard, P. G.; Nichols, M. A. *J. Am. Chem. Soc.* **1993**, *115*, 6262. (c) Jackman, L. M.; Smith, B. D. *J. Am. Chem. Soc.* **1988**, *110*, 3829. (d) Jackman, L. M.; DeBrosse, C. W. *J. Am. Chem. Soc.* **1987**, *109*, 5355.

(13) Williard, P. G.; Liu, Q. *J. Org. Chem.* **1994**, *59*, 1596.

(14) Schriver, D. F.; Drezden, M. A. *The Manipulation of Air-Sensitive Compounds*; Wiley: New York, 1986.

(15) Chisholm, M. H.; Drake, S. R.; Naiini, A. A.; Streib, W. E. *Polyhedron* **1991**, *10*, 337.

(16) Deck, P. A. *Chem. Eng. News* **2005**, *83*, 8.

Table 1. Crystallographic Data for Compounds **1**−**6**

	1	**2**	**3**	**4**	**5**	**6**
formula	$C_{26}H_{28}F_3K_3O_7$	$C_{30}H_{36}I_3K_3O_9$	$C_{30}H_{36}I_3O_9Rb_3$	$C_{22}H_{20}Cl_3K_3O_5$	$C_{22}H_{20}Br_3K_3O_5$	$C_{50}H_{60}Br_5O_{15}Rb_5$
formula wt	626.78	1038.59	1177.70	588.03	721.41	1727.88
T (K)	100(2)	100(2)	100(2)	100(2)	100(2)	100(2)
crystal system	monoclinic	monoclinic	monoclinic	monoclinic	orthorhombic	monoclinic
space group	$P2_1/c$	$P2_1/c$	$P2_1/c$	$P2_1/c$	$Pnma$	$P2_1/c$
a (Å)	13.1101(5)	11.2104(8)	11.6779(11)	18.0451(8)	7.1981(4)	9.1298(6)
b (Å)	19.5138(7)	15.3230(12)	15.7238(14)	21.0177(10)	17.5149(8)	30.9592(16)
c (Å)	11.76.26(5)	22.0706(18)	21.4171(19)	7.0816(3)	21.2140(10)	21.3492(12)
α (deg)	90	90	90	90	90	90
β (deg)	105.4(2)	103.706(4)	103.589(5)	91.869(3)	90	93.446(3)
γ (deg)	90	90	90	90	90	90
V (Å^3)	2901.2(2)	3683.3(5)	3822.5(6)	2684.4(2)	2671.5(2)	6023.5(6)
Z	4	4	4	4	4	4
density (Mg/m^3)	1.435	1.873	2.046	1.455	1.792	1.903
μ (λ) (mm^{-1})	0.531	2.932	6.294	0.836	5.022	7.411
crystal size (mm^{-1})	0.18 × 0.27 × 0.28	0.17 × 0.19 × 0.30	0.23 × 0.28 × 0.33	0.12 × 0.12 × 0.38	0.13 × 0.19 × 0.33	0.17 × 0.21 × 0.34
θ range (deg)	1.92−32.03	1.87−29.57	1.96−28.70	1.13−25.68	1.92−27.10	1.63−25.03
T_{max}/T_{min}	0.91/0.87	0.63/0.47	0.31/0.16	0.91/0.74	0.57/0.29	0.35/0.20
no. of reflns collected	171979	162736	52499	36932	54582	38586
no. of independent reflns	10110	10342	4942	5088	3050	10620
no. of observed reflns [$I > 2\sigma(I)$]	8418	8741	4057	4390	2614	7579
GOF on F^2	1.017	1.040	1.079	1.183	1.082	1.003
R1, wR2 [$I > 2\sigma(I)$]	0.0292, 0.0721	0.0223, 0.0439	0.0349, 0.0815	0.0664, 0.1673	0.0245, 0.0517	0.0391, 0.0666
R1, wR2 (all data)	0.0398, 0.0775	0.0313, 0.0463	0.0501, 0.0894	0.0754, 0.1731	0.0347, 0.0558	0.0710, 0.0745
largest peak/hole (e Å^{-3})	0.500/−0.417	0.897/−0.851	0.981/−0.802	1.488/−0.527	0.695/−0.430	0.845/−0.616

diffractometer equipped with an Oxford Cryosystems 700 series low-temperature apparatus. Cell parameters were determined using reflections harvested from three sets of 20 0.3° ω scans. The orientation matrix derived from this was passed to COSMO to determine the optimum data collection strategy.[17] Cell parameters were refined using reflections with $I \geq 10\sigma(I)$ harvested from the entire data collection. All data were corrected for Lorentz and polarization effects as well as for absorption. Table 1 lists the key crystallographic parameters for **1**−**6**. The structures were solved and refined using SHELXTL.[18] Structure solution was by direct methods. Non-hydrogen atoms not present in the direct methods solution were located by successive cycles of full-matrix least-squares refinement on F^2 followed by the calculation of a difference Fourier map. All non-hydrogen atoms were refined with parameters for anisotropic thermal motion. Hydrogen atoms were placed at idealized geometries and allowed to ride on the position of the parent atom. Hydrogen thermal parameters were set to 1.2 times the equivalent isotropic unit of the parent atom and 1.5 times for methyl hydrogens.

Synthesis of [(4-F-C$_6$H$_4$OK)$_6$·(dioxane)$_4$]$_\infty$ (1). KHMDS (3 mmol, 598 mg) was added to a stirred solution of 4-F-C$_6$H$_4$OH (3 mmol, 340 mg) in dioxane (20 mL). A white precipitate formed that completely dissolved on heating the solution to reflux. X-ray quality crystals were obtained by slowly cooling the resulting solution in a hot water bath. Crystalline yield: 90 mg, 69.2%. ^{1}H NMR (d_6-DMSO, 293 K): δ_H 3.56 (s, CH$_2$, dioxane), 5.98 (m, 12H, *o*-H, Ar), 6.49 (m, 12H, *m*-H, Ar).

Synthesis of [(4-I-C$_6$H$_4$OK)$_6$·(dioxane)$_6$]$_\infty$ (2). KHMDS (3 mmol, 598 mg) was added to a stirred solution of 4-I-C$_6$H$_4$OH (3 mmol, 660 mg) in dioxane (16 mL). A white precipitate formed that completely dissolved on heating the solution to reflux. X-ray quality crystals were obtained by slowly cooling the resulting solution in a hot water bath. Crystalline yield: 220 mg, 60.1%. ^{1}H NMR (d_6-DMSO, 293 K): δ_H 3.56 (s, CH$_2$, dioxane), 5.86 (d, $^3J_{H,H}$ = 8.0 Hz, 12H, *o*-H, Ar), 6.83 (d, $^3J_{H,H}$ = 8.0 Hz, 12H, *m*-H, Ar).

Synthesis of [(4-I-C$_6$H$_4$ORb)$_6$·(dioxane)$_6$]$_\infty$ (3). [^{t}BuORb·^{t}BuOH]$_\infty$ (1 mmol, 230 mg) was added to a stirred solution of 4-I-C$_6$H$_4$OH (1 mmol, 220 mg) in dioxane (9 mL). A white precipitate formed that completely dissolved on heating the solution to reflux. X-ray quality crystals were obtained by slowly cooling the resulting solution in a hot water bath. Crystalline yield: 260 mg, 84.7%. ^{1}H NMR (d_6-DMSO, 293 K): δ_H 3.56 (s, CH$_2$, dioxane), 5.84 (d, $^3J_{H,H}$ = 8.0 Hz, 12H, *o*-H, Ar), 6.80 (d, $^3J_{H,H}$ = 8.0 Hz, 12H, *m*-H, Ar).

Synthesis of [(4-Cl-C$_6$H$_4$OK)$_3$·(dioxane)]$_\infty$ (4). KHMDS (3 mmol, 598 mg) was added to a stirred solution of 4-Cl-C$_6$H$_4$OH (3 mmol, 390 mg) in dioxane (10 mL). A white precipitate formed that completely dissolved on heating the solution to reflux. X-ray quality crystals were obtained by slowly cooling the resulting solution in a hot water bath. Crystalline yield: 480 mg, 81.8%. ^{1}H NMR (d_6-DMSO, 293 K): δ_H 3.56 (s, CH$_2$, dioxane), 5.94 (d, $^3J_{H,H}$ = 8.0 Hz, 6H, *o*-H, Ar), 6.55 (d, $^3J_{H,H}$ = 8.0 Hz, 6H, *m*-H, Ar).

Synthesis of [(4-Br-C$_6$H$_4$OK)$_2$·(dioxane)$_{0.5}$]$_\infty$ (5). KHMDS (3 mmol, 598 mg) was added to a stirred solution of 4-Br-C$_6$H$_4$OH (3 mmol, 520 mg) in dioxane (15 mL). A white precipitate formed that completely dissolved on heating the solution to reflux. X-ray quality crystals were obtained by slowly cooling the resulting solution in a hot water bath. Crystalline yield: 250 mg, 32.9%. ^{1}H NMR (d_6-DMSO, 293 K): δ_H 3.56 (s, CH$_2$, dioxane), 5.92 (d, $^3J_{H,H}$ = 8.0 Hz, 4H, *o*-H, Ar), 6.69 (d, $^3J_{H,H}$ = 8.0 Hz, 4H, *m*-H, Ar).

Synthesis of [(4-Br-C$_6$H$_4$ORb)$_5$·(dioxane)$_5$]$_\infty$ (6). [^{t}BuORb·^{t}BuOH]$_\infty$ (1 mmol, 230 mg) was added to a stirred solution of 4-Br-C$_6$H$_4$OH (1 mmol, 173 mg) in dioxane (14 mL) and hexane (14 mL). A white precipitate formed that completely dissolved on heating the solution to reflux. X-ray quality crystals were obtained by slowly cooling the resulting solution in a hot water bath. Crystalline yield: 150 mg, 43.5%. ^{1}H NMR (d_6-DMSO, 293 K): δ_H 3.56 (s, CH$_2$, dioxane), 5.88 (d, $^3J_{H,H}$ = 8.0 Hz, 10H, *o*-H, Ar), 6.28 (d, $^3J_{H,H}$ = 8.0 Hz, 10H, *m*-H, Ar).

Results and Discussion

Crystals of six complexes were successfully prepared, following the reaction of either potassium hexamethyldisilazide or the rubidium base [^{t}BuORb·^{t}BuOH]$_\infty$ with the

(17) Kaercher, J. *COSMO*; Bruker-Nonius AXS, Inc.: Madison, WI, 2003.
(18) Sheldrick, G. M. *SHELXTL*; University of Göttingen: Göttingen, Germany, 2001.

Table 2. Key Bond Lengths (Å) and Bond Angles (deg) for **1**−**6**[a]

	$M-O_{Ar}$	$M-O_{diox}$	$O_{Ar}-M-O_{Ar}$	$M-O_{Ar}-M$
1 (M = K)	2.5997(7)−2.28602(7) <2.7129>	2.7021(8)−2.7656(9) <2.7244>	84.10(2)−168.99(2) <95.43>	85.12(2)−175.41(3) <98.04>
2 (M = K)	2.623(1)−2.895(1) <2.711>	2.781(1)−2.831(1) <2.805>	82.27(2)−175.18(4) <95.62>	91.14(4)−113.18(5) <97.85>
3 (M = Rb)	7.737(4)−2.847(4) <2.805(4)>	2.855(4)−2.997(5) <2.928>	77.45(12)−172.45(12) <92.89>	88.55(15)−173.73(15) <101.33>
4 (M = K)	2.668(3)−2.877(3) <2.756>	2.682(3)	77.49(10)−161.64(11) <98.75>	77.67(9)−152.53(15) <104.28>
5 (M = K)	2.675(2)−2.866(2) <2.755>	2.695(1)	73.51(4)−161.09(3) <102.01>	75.74(3)−149.51(8) <99.66>
6 (M = Rb)	2.774(3)−3.016(3) <2.899>	3.089(4)−3.329(3) <3.209>	70.05(9)−162.22(9) <93.20>	82.09(8)−173.3(1) <102.2>

[a] Mean parameters are shown in angle brackets.

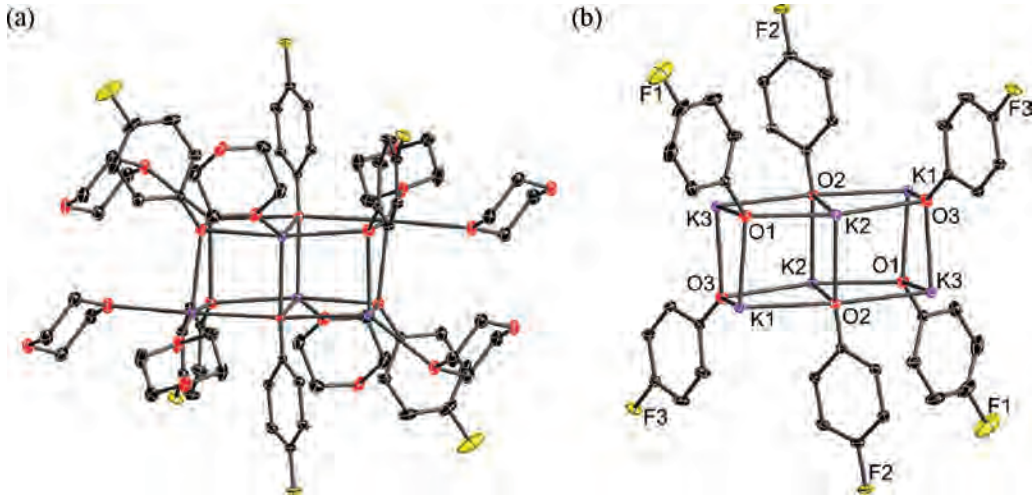

Figure 2. Section of the crystal structure of **1** showing (a) the full hexameric aggregate with eight-coordinated dioxane molecules and (b) the hexameric aggregate with dioxane molecules removed for clarity.

appropriate phenol using dioxane as the solvent medium. The crystal structures obtained can be classified into two groups: (i) $[(4\text{-F-}C_6H_4OK)_6\cdot(\text{dioxane})_4]_\infty$ (**1**), $[(4\text{-I-}C_6H_4OK)_6\cdot(\text{dioxane})_6]_\infty$ (**2**), and $[(4\text{-I-}C_6H_4ORb)_6\cdot(\text{dioxane})_6]_\infty$ (**3**) that form discreet M_6O_6 hexameric aggregates connected through dioxane; and (ii) $[(4\text{-Cl-}C_6H_4OK)_3\cdot(\text{dioxane})]_\infty$ (**4**), $[(4\text{-Br-}C_6H_4OK)_2\cdot(\text{dioxane})_{0.5}]_\infty$ (**5**), and $[(4\text{-Br-}C_6H_4ORb)_5\cdot(\text{dioxane})_5]_\infty$ (**6**) that form 1D inorganic rods coordinated by dioxane. The local and extended structures of **1**−**3** will be discussed first followed by an analysis of the organic−inorganic hybrid materials **4**−**6**. A summary of comparative bond lengths and bond angles for **1**−**6** is reported in Table 2.

Frameworks from Discreet SBUs. The molecular component of $[(4\text{-F-}C_6H_4OK)_6\cdot(\text{dioxane})_4]_\infty$ (**1**) is composed of a prismatic, hexameric potassium aryloxide aggregate (Figure 2). There are three different bonding environments for the metal ions within **1**. The terminal metal, K1, is coordinated by two dioxane molecules as well as a fluoride atom from a neighboring aggregate. The interaggregate $K1-F_{Ar}$ distance in **1** is 2.7385(7) Å, which is well within the expected range for such an interaction.[19] As a comparison, the $K-O_{diox}$ distances in **1** range between 2.7021(8) and 2.7656(9) Å. The second terminal potassium, K3, is coordinated by only one dioxane molecule and one fluoride from a neighboring aggregate with a $K3-F_{Ar}$ distance of 2.7948(7) Å. Finally, the central potassium, K2, is coordinated by only one dioxane molecule with no close K−F interactions present. Thus, both F1 and F2, and their symmetry equivalents, bridge to neighboring aggregates. In comparison, only the two fluorides in the middle of the aggregate act as bridges to other aggregates for the smaller sodium analogue.[6b]

Overall, with eight dioxane molecules bridging to other aggregates plus the eight interaggregate $K-F_{Ar}$ interactions, the hexameric aggregate in **1** acts as a 16-connected node (panels a and b of Figure 3). Examination of the extended structure shows that each node actually binds to eight unique neighbors, where each aggregate is involved in double-bridging interactions (Figure 3c). Specifically, there are three different types of double bridges present. The first is a double dioxane bridge, which has been seen before in other high-connectivity networks reported by our group.[9] This type of bridge accounts for two of the total points of extension in the net. The second double bridge uses one dioxane molecule and one $K-F_{Ar}$ interaction, which accounts for four of the total points of extension. An example of this type of bridge is observed when F3 coordinates to K3 of a neighboring aggregate, while the dioxane molecule coordinates to K2 bridges of a neighboring aggregate. Finally, two points of extension in the net exist because of $K-F_{Ar}$ double bridges. This third double bridge is seen with K1 of two neighboring aggregates binding through two F2 atoms.

Although the bridging between aggregates is unique, the eight-connected node gives an extended structure with **bcu** topology (Figure 3c). This topology is somewhat unusual in terms of the number of connections present (i.e., greater than six), but this highly symmetric net has now been seen multiple times in our own work and in others.[20] The formation of a hexamer is also consistent with our previous characterization of the sodium analogue $[(4\text{-F-}C_6H_4ONa)_6\cdot(\text{dioxane})_3]_\infty$, but the larger potassium

(19) Allen, F. H. *Acta Crystallogr.* **2002**, *B58*, 380.

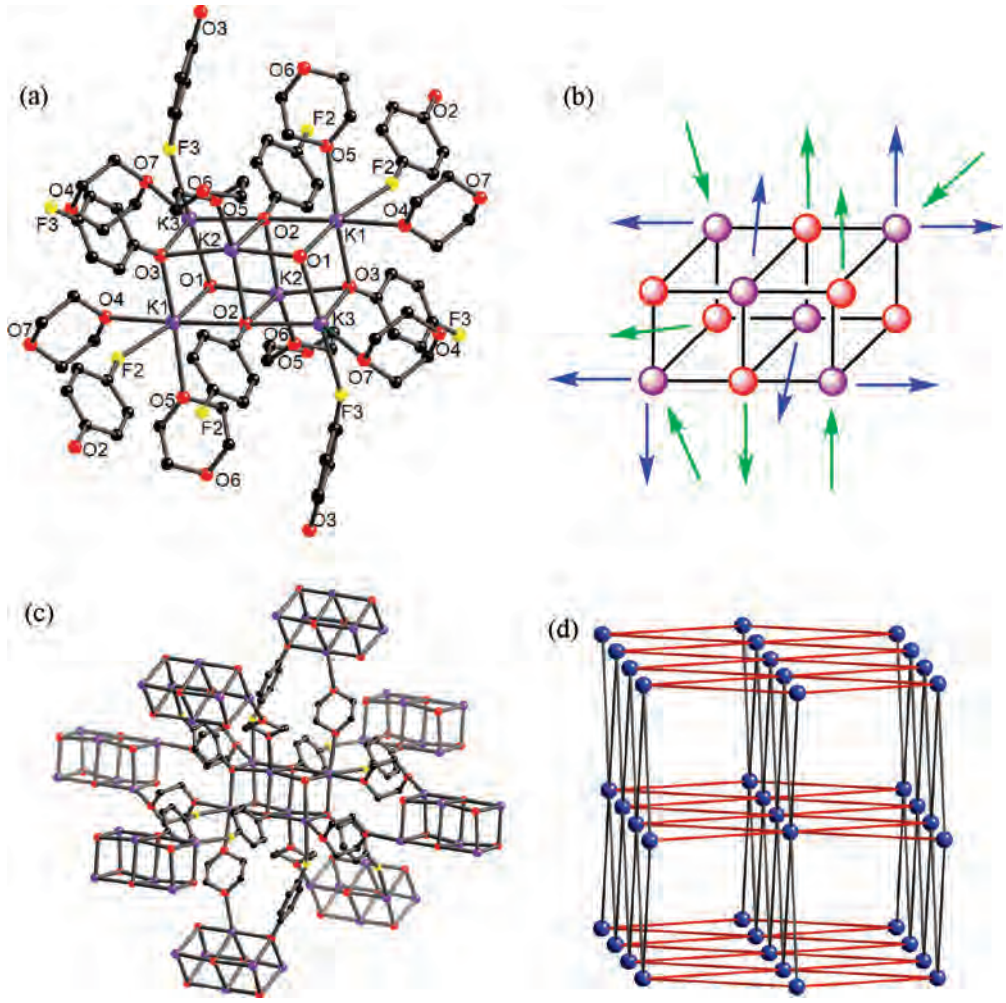

Figure 3. Structure of **1** showing (a) the hexameric aggregate with the eight, bridging dioxane molecules as well as the eight aryloxide ligands that bridge through $K-F_{Ar}$ interactions; (b) an illustration of the aggregate with the eight, bridging dioxane molecules (blue arrows) and eight bridging aryl ligands (green arrows); (c) the hexameric aggregate bridged to neighboring aggregates through eight double bridges; and (d) the extended structure with **bcu** topology, where the hexameric aggregates are represented as blue spheres.

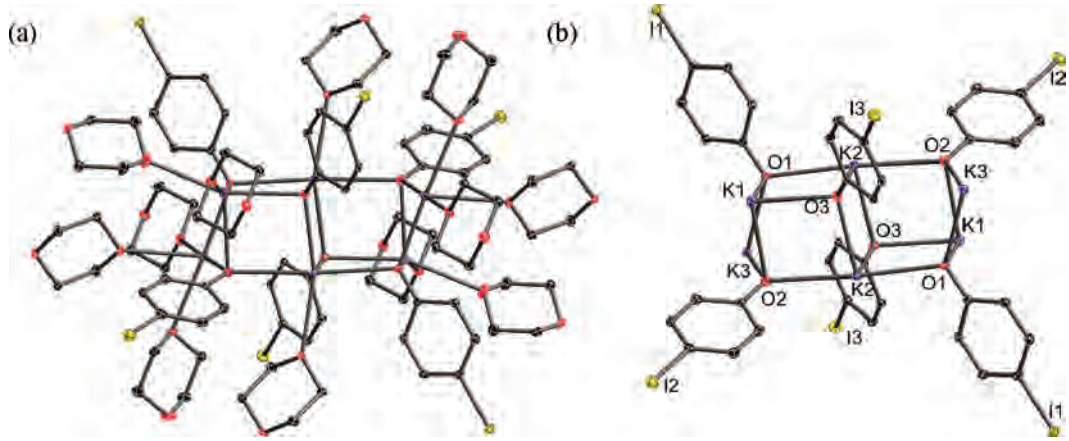

Figure 4. Structure of **2** showing (a) the full hexameric aggregate with 12-coordinated dioxane molecules and (b) the hexameric aggregate with dioxane molecules removed for clarity.

metal ions allow solvation by eight, rather than six, dioxane molecules.[6]

The potassium and rubidium aggregates of the iodo-substituted phenoxide, $[(4\text{-I-}C_6H_4OK)_6\cdot(\text{dioxane})_6]_\infty$ (**2**) and $[(4\text{-I-}C_6H_4ORb)_6\cdot(\text{dioxane})_6]_\infty$ (**3**), form similar hexamers, consisting of triple stacks of dimers coordinated by 12 dioxane molecules (Figure 4). The hexameric aggregates in both **2** and **3** differ from those in **1** by having a pair of elongated outer edges. This is particularly apparent in **2** where the two K3−O3 distances in the aggregate are greater than 4 Å, whereas the rest of the $K-O_{Ar}$ distances are within the range 2.623(1)−2.895(1) Å [mean 2.711(1) Å]. In the rubidium analogue, **3**, the two outer edges are 3.193 Å, whereas the remaining

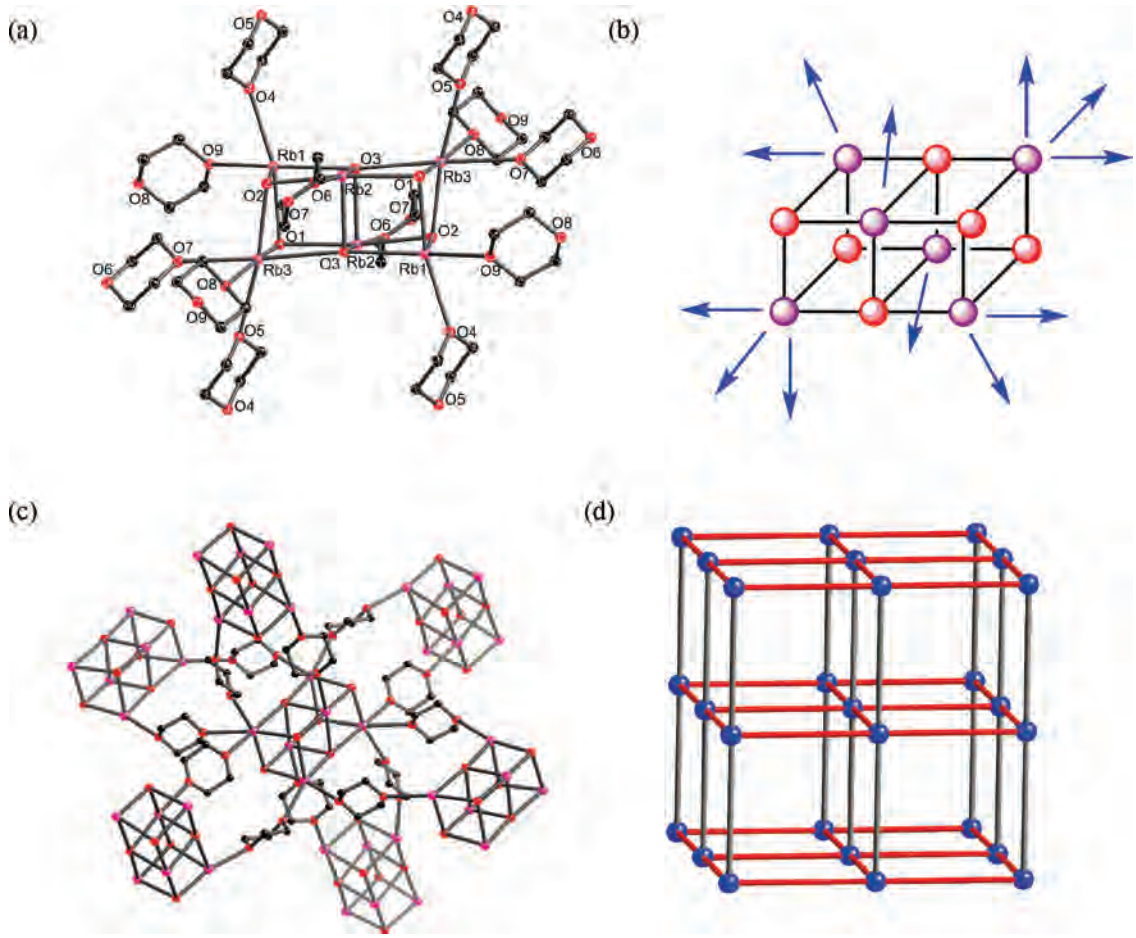

Figure 5. Structure of **3** showing (a) the hexameric aggregate coordinated by twelve bridging dioxane molecules, (b) an illustration of the aggregate showing the twelve bridging dioxane molecules (blue arrows), (c) the hexameric aggregate bridged to neighboring aggregates through six dioxane double bridges, and (d) the extended structure with **pcu** topology, where the hexameric aggregates are represented as blue spheres.

Rb−O_{Ar} distances range between 2.737(4) and 2.847(4) Å [mean 2.805(4) Å]. This structural type is unusual but not unprecedented. The pyridine solvate of potassium 2-methylphenoxide [(2-Me-$C_6H_4OK)_6$·$(py)_4$] has two independent, hexameric aggregates in the asymmetric unit that are both tetrasolvated by pyridine.[21] One aggregate has two open edges, while the second aggregate has the more commonly seen closed triple stack of dimers motif. Also, the mixed-metal enolate species $\{H_2C{=}C(^tBu)O\}_6Li_2Na_4$·$(^iPrNH)_2$] has an analogous structural arrangement. In this complex, two of the terminal sodium metal ions of the stack are solvated by di-isopropylamine and form close contacts with the enolate double bonds rather than binding to adjacent enolate oxygen atoms.[22] From our own work, we have observed the change from triple stacks of dimers to prismatic hexamers upon encapsulation of a water molecule.[7d] More specifically, this structural change involves the opening of two central M−X interactions to give a drum-shaped aggregate. A common feature in **2** and **3** is that the open edges involve metal ions that are coordinated by three dioxane molecules. Indeed, to our knowledge **2** and **3** are the first characterized examples of hexameric alkali metal aggregates containing trisolvated metal ions.[9,21,23] Clearly, the K−O_{diox} interactions will weaken the accompanying K−O_{Ar} interactions, and this is likely the reason for the opening of the two edges of the triple stack.

Another significant difference between the structures of **2** and **3**, and that of **1**, is that the metal ions no longer have close contacts to the halides of adjacent aggregates. For example, in **2** the interaggregate K−I distances are greater than 3.9 Å, which are substantially longer than the K1−F_{Ar} distances of 2.7385(7) and 2.7948(7) Å in **1**. Interestingly, the metals in all three complexes **1**−**3** are coordinated by the same total number of Lewis bases. However, in **1** four of the potassiums have a K−F_{Ar} interaction, but in **2** and **3** this coordination has been replaced by dioxane solvation. Therefore, there are still three different coordination environments for the metals in **2** and **3**, but now K1 (Rb1) is coordinated by two dioxane molecules, K2 (Rb2) is coordinated by one dioxane molecule, and K3 (Rb3) is coordinated by three molecules of dioxane for a total of 12 dioxane molecules solvating the aggregate. It appears likely that the high electronegativity of the fluoride promotes the formation of the interaggregate interactions in **1**.

The extended frameworks of **2** and **3** are isostructural. The hexameric aggregates are coordinated by a total of 12 dioxane molecules (panels a and b of Figure 5). Each aggregate links to six neighboring aggregates through dioxane double

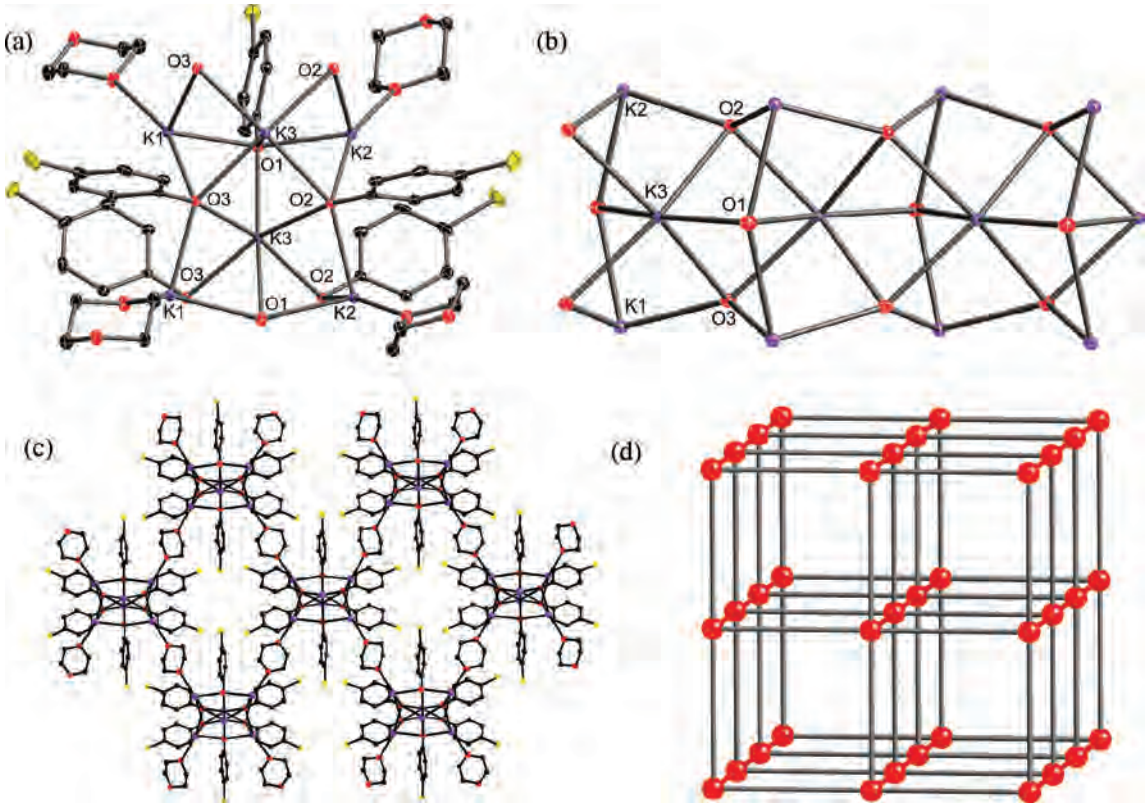

Figure 6. Structure of **4** showing (a) a slice of the 1D inorganic rod; (b) a simplified view of the inorganic chain displaying only the $K-O_{Ar}$ interactions; (c) an expanded view looking down the 1D rods, highlighting the bridging by dioxane to give parallel stacks of 4^4-nets; and (d) the **pcu** net with the inorganic rods represented in red and the dioxane bridges in gray.

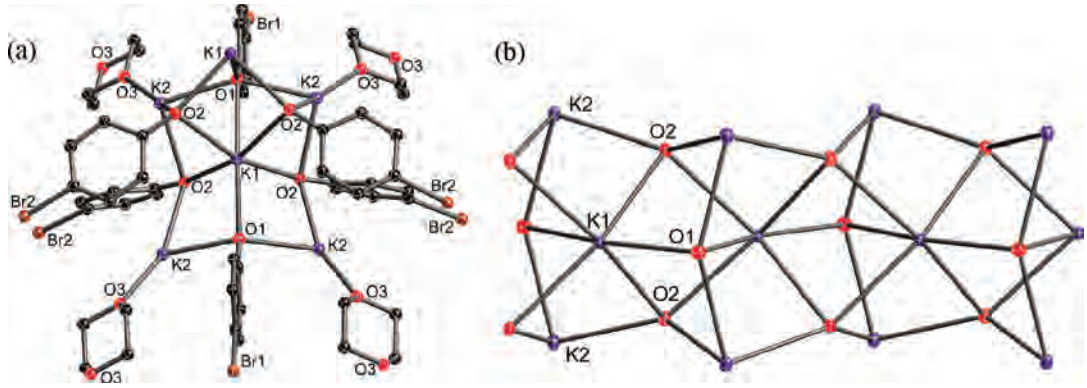

Figure 7. Structure of **5** showing (a) a slice of the 1D inorganic rod and (b) a simplified view of the inorganic chain showing only the $K-O_{Ar}$ interactions.

bridges. For example, K3 (Rb3) and K1 (Rb1) bridge through dioxane to K2 (Rb2) and K3 (Rb3) of a neighboring aggregate (Figure 5c). These are the first compounds within our extended framework series that display solely double dioxane bridge linkages. Overall, each SBU in **2** and **3** connects to six unique neighbors through double bridges, resulting in six-connected nets with primitive cubic (**pcu**) topology (Figure 5d).

Frameworks from Inorganic Rods. To our surprise, the solid-state structures of the chloro- and bromo-substituted derivatives $[(4\text{-Cl-}C_6H_4OK)_3\cdot(\text{dioxane})]_\infty$ (**4**), $[(4\text{-Br-}C_6H_4\text{-}OK)_2\cdot(\text{dioxane})_{0.5}]_\infty$ (**5**), and $[(4\text{-Br-}C_6H_4ORb)_5\cdot(\text{dioxane})_5]_\infty$ (**6**) did not contain molecular SBUs as anticipated. Instead, each structure is built from 1D inorganic rods, consisting of $M-O_{Ar}$ interactions.

The asymmetric unit of **4** is composed of a 4-Cl-C_6H_4OK trimeric unit, where two of the potassium atoms are coordinated by dioxane. Symmetry expansion of the asymmetric shows that the potassium aryloxide does not form a discreet SBU but rather builds an inorganic rod from $K-O_{Ar}$ interactions (panels a and b of Figure 6). There are two different bonding environments for the metal ions in **4**. Both K1 and K2 are coordinated by a dioxane molecule and by three μ_4-aryloxide oxygen atoms. The potassium in the center of the inorganic rod, K3, is pseudo-octahedrally coordinated by six μ_4-aryloxide oxygen atoms. This leads to significant differences in the $K-O_{Ar}$ bond distances around K3. There are three short $K-O_{Ar}$ bond distances on one face of the octahedron [ranging between 2.668(3) and 2.702(3) Å] and three

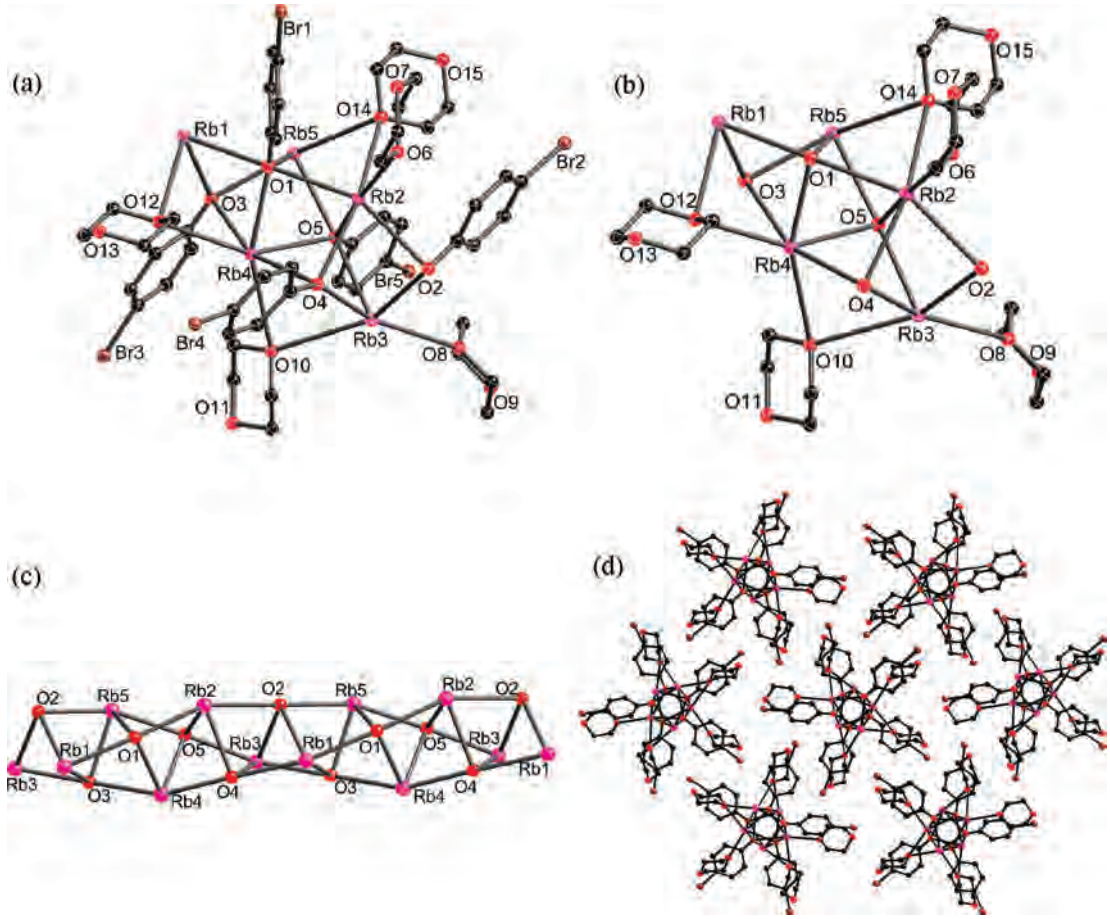

Figure 8. Structure of **6** showing (a) a slice of the extended inorganic structure formed through K−O_{Ar} interactions, (b) a simplified view highlighting the K−O_{Ar} and K−O_{diox} interactions, (c) a view of the helical 1D rod, and (d) a view of the hexagonally packed rods.

substantially longer K−O_{Ar} interactions [ranging between 2.791(3) and 2.877(3) Å] on the second face.

In **4**, each inorganic rod is linked to four other rods through dioxane bridges to give an extended structure with parallel stacks of 4^4-nets (Figure 6c). Therefore, the network can be described also as an organic−inorganic hybrid material with a **pcu**-type rod packing.[5b]

The potassium 4-bromophenoxide analogue, $[(4\text{-Br-}C_6H_4OK)_2\cdot(\text{dioxane})_{0.5}]_\infty$ (**5**), adopts a structure very similar to that of **4**. The asymmetric unit of **5** is composed of a 4-Br-C_6H_4OK dimeric unit, where one of the potassium atoms, K2, is coordinated by a molecule of dioxane. This leads to only two unique potassium environments in **5** (space group *Pnma*) compared with the three different types of metal ions in **4** (space group $P2_1/c$). Apart from this change, the local and extended structures, **4** and **5**, are essentially isostructural (Figure 7).

The asymmetric unit of the rubidium analogue $[(4\text{-Br-}C_6H_4ORb)_5\cdot(\text{dioxane})_5]_\infty$(**6**) is composed of a pentameric unit with each metal solvated by one dioxane. Symmetry expansion of the asymmetric unit gives a 1D, inorganic rod built from Rb−O_{Ar} interactions (Figure 8a). The rod core in **6** differs from those in **4** and **5**. All of the aryloxide oxygen atoms in the structure are μ_4-bridges, and there are three different bonding environments for the five rubidium ions. All of the metals are coordinated by four μ_4-aryloxide oxygen atoms, but the nature of the dioxane coordination varies between the metals. There are two types of coordinated dioxane in the structure, the common μ_1 form and also a second μ_2 form, where the oxygen of the dioxane bridges between two metals (Figure 8b). This type of μ_2-bridge has been seen numerous times for tetrahydrofuran (THF)-solvated complexes but has not been previously reported for dioxane.[24] In terms of the rubidium environments, both Rb1 and Rb5 are coordinated by one μ_2-dioxane, while Rb2 and Rb3 are coordinated by one μ_1-dioxane and one μ_2-dioxane, and Rb4 is coordinated by two μ_2-dioxane molecules.

Unlike the extended inorganic rods of **4** and **5**, those in **6** are not bridged through dioxane. The closest contacts

(20) (a) Long, D.-L.; Blake, A. J.; Champness, N. R.; Wilson, C.; Schröder, M. *Angew. Chem., Int. Ed.* **2001**, *40*, 2443. (b) Luo, T.-T.; Tsai, H.-L.; Yang, S.-L.; Liu, Y.-H.; Yadav, R. D.; Su, C.-C.; Ueng, C.-H.; Lin, L.-G.; Lu, K.-L. *Angew. Chem., Int. Ed.* **2005**, *44*, 6063. (c) Zhang, X.-M.; Fang, R.-Q.; Wu, H.-S. *J. Am. Chem. Soc.* **2005**, *127*, 7670. (d) Li, D.; Wu, T.; Zhou, X.-P.; Zhou, R.; Huang, X.-C. *Angew. Chem., Int. Ed.* **2005**, *44*, 4175. (e) Fang, Q.-R.; Zhu, G.-S.; Jin, Z.; Xue, M.; Wei, X.; Wang, D.-J.; Qiu, S.-L. *Angew. Chem., Int. Ed.* **2006**, *45*, 6126. (f) Zhang, J.; Kang, Y.; Zhang, J.; Li, Z.-J.; Qin, Y.-Y.; Yao, Y.-G. *Eur. J. Inorg. Chem.* **2006**, 2253.
(21) Boyle, T. J.; Andrews, N. L.; Rodriguez, M. A.; Campana, C.; Yiu, T. *Inorg. Chem.* **2003**, *42*, 5357.
(22) Henderson, K. W.; Williard, P. G.; Bernstein, P. R. *Angew. Chem., Int. Ed. Engl.* **1995**, *34*, 1117.
(23) For a related Mn structure see: Godbole, M. D.; Roubeau, O.; Mills, A. M.; Kooijman, H.; Spek, A. L.; Bouwman, E. *Inorg. Chem.* **2006**, *45*, 6713.
(24) For a recent example see: Chivers, T.; Fedorchuck, C.; Parvez, M. *Inorg. Chem.* **2004**, *43*, 2643.

involving the metals between neighboring rods are Rb−Br_{Ar} interactions that are still greater than 4 Å apart.[25] Each rod is surrounded by six others in a hexagonal packing array (Figure 8d). One final note of interest is that the rods are helical (Figure 8c). Alternating rods in the extended packing have left- and right-handedness, giving achiral space group $P2_1/c$. The rod shown in Figure 8c has a left-handed helical twist.

Conclusions

The characterizations of **1**−**6** demonstrate that potassium and rubidium *p*-halide-substituted aryloxides can readily be used in the synthesis of coordination frameworks. The extended structures are notable on several fronts. First, the network of **1** is constructed from two types of interactions: dioxane bridges and close K−F_{Ar} interactions. From our studies thus far, only the fluoride complexes contain metal−halide interactions.[6b] This is presumably related to the higher electronegativity of fluorine compared with those of the remaining halides and consequently its greater ability to form stronger interactions with the highly electropositive alkali metal ions.

Next, the combination of large, unsaturated metal ions incorporated within hexametallic cages in **1**−**3** allows for multiple points for network extension from the aggregated SBUs. In turn, this results in the formation of high connectivity networks. Compound **1** has 16 connections between each aggregate and its neighbors, whereas compounds **2** and **3** form isostructural 12-connected nets. A feature of these nets is that they all incorporate double bridges, such that the extended nets form the highly symmetric **bcu** and **pcu** topologies.[3]

Finally, the unanticipated formation of 1D inorganic rods built solely from M−O_{Ar} interactions was found, following the syntheses of **4**−**6**. In **4** and **5**, the rods act as 1D SBUs and are cross-linked by bridging dioxane molecules to form **pcu** nets. Compound **6** contains only terminally solvating dioxane with the 1D rods close packing the solid state but not formally cross-linking. This is the first set of alkali metal aryloxide complexes prepared by our group that do not form molecular SBUs.[6] Examples of alkali metal aryloxides forming polymeric materials have been previously reported; however, these are normally found in the absence of donor solvents or for functionalized aryloxides.[21,26] As far as we are aware, the two types of M−X−M polymeric connectivities observed within the 1D rods of **4**−**6** are novel.[19] However, the **pcu**-type rod packing has been previously observed in dicarboxylate metal−organic frameworks (MOFs).[5b] It is unclear at this point why complexes **4**−**6** form inorganic rods rather than discrete aggregates. Further studies will be focused on addressing this question by expanding on this library of structures. However, the characterization of **4**−**6** demonstrates that certain alkali metal complexes may be useful in building hybrid organic−inorganic materials. Such hybrid complexes are interesting from an application standpoint because the extended inorganic component should provide additional stability to the framework.[4]

Acknowledgment. We gratefully acknowledge the Petroleum Research Fund (41716-AC3) and the National Science Foundation (CHE-0443233) for instrumentation support.

Supporting Information Available: Crystallographic data for compounds **1**−**6** in CIF format. This material is available free of charge via the Internet at http://pubs.acs.org.

IC801140U

(25) For examples of K−Br interactions see: (a) Helgesson, G.; Jagner, S. *J. Chem. Soc., Dalton Trans.* **1993**, 1069. (b) Rusanova, J. A.; Domasevitch, K. V.; Vassilyeva, O. Y.; Kokozay, V. N.; Rusanov, E. B.; Nedelko, S. G.; Chukova, O. V.; Ahrens, B.; Raithby, P. R. *J. Chem. Soc., Dalton Trans.* **2000**, 2157. (c) Ahmad, R.; Hardie, M. J. *New J. Chem.* **2004**, *28*, 1315. (d) Ahmad, R.; Franken, A.; Kennedy, J. D.; Hardie, M. J. *Chem.−Eur. J.* **2004**, *10*, 2190. (e) Kitanovski, N.; Golic, L.; Meden, A.; Ceh, B. *Croat. Chem. Acta* **2005**, *78*, 111.

(26) For examples see: (a) Couhorn, U.; Dronskowski, R. *Z. Anorg. Allg. Chem.* **2004**, *630*, 427. (b) Couhorn, U.; Dronskowski, R. *Z. Anorg. Allg. Chem.* **2003**, *629*, 647. (c) Couhorn, U.; Dronskowski, R. *Z. Anorg. Allg. Chem.* **2003**, *629*, 2554. (d) Harrowfield, J. M.; Sharma, R. P.; Shand, T. M.; Skelton, B. W.; White, A. H. *Aust. J. Chem.* **1998**, *51*, 707. (e) Harrowfield, J. M.; Sharma, R. P.; Skelton, B. W.; White, A. H. *Aust. J. Chem.* **1998**, *51*, 723. (f) Harrowfield, J. M.; Sharma, R. P.; Skelton, B. W.; White, A. H. *Aust. J. Chem.* **1998**, *51*, 747. (g) Dinnebier, R. E.; Pink, M.; Sieler, J.; Stephens, P. W. *Inorg. Chem.* **1997**, *36*, 3396. (h) Dinnebier, R. E.; Pink, M.; Sieler, J.; Stephens, P. W. *Inorg. Chem.* **1997**, *36*, 3398.